

A High-Speed Towing Tank for Hydrodynamics and Cavitation Experiments

**Hong-Hui Shi¹, Bo Chen¹, Martin Brouillette², Xiao-Ping Zhang¹
and Li-Bing Peng¹**

¹Dept. of Fluids Engineering, College of Mechanical Engineering & Automation,
Zhejiang Sci-Tech University, Hangzhou 310018, Zhejiang Province, China

²Dept. of Mechanical Engineering, University of Sherbrooke, Sherbrooke J1K 2R1,
Quebec Province, Canada
E-mail: hhshi@zstu.edu.cn

Abstract

This article presents a new type of high-speed towing tank developed at Zhejiang Sci-Tech University, China. The towing tank can be used to do hydrodynamics and cavitation experiments effectively and can ensure high repeatability. Two groups of test models with square and circular cross-sectional areas were applied to test the hydrodynamic characteristics of the high-speed towing tank. The maximum velocity of the test models can reach about 18 m/s. It was found that the velocities and the cavitating wakes of the models are related to the shape of the model. This paper's work gives a method that how to improve traditional towing tank.

Keywords: High-speed towing tank; Hydroballistic behavior; Wake cavitation; Model geometry

1. INTRODUCTION

The Bernoulli's equation in fluid mechanics tells us that when fluid velocity increases, fluid static pressure decreases. In liquid, if fluid pressure becomes lower than the saturation vapor pressure, cavity appears. It is commonly to use cavitation number σ to ascertain whether a cavity occurs and how severe the cavitation is when liquid flows around an object. σ is defined as:

$$\sigma = \frac{P_{\infty} - P_v}{0.5\rho V^2} \quad (1)$$

where P_{∞} is undisturbed fluid pressure, P_v is cavity pressure, ρ and V are fluid density and velocity respectively. If fluid velocity is high enough, then the object can be completely enclosed by a cavity which is called supercavity [1].

In 1895, Sir Charles Parsons invented the first water tunnel to study cavitation problems with propellers [2]. Today, there have been many modern water tunnels over the world [3]. However, in order to deeply investigate cavitation phenomenon, new experimental method and device are needed.

Towing tank is a very useful tool to study hydrodynamics of ships and underwater vehicles. The disadvantage of conventional towing tanks is that the towing velocity is low and has usually only a few meters per second [4-5]. Therefore, towing tank is not suitable for cavitation research, especially natural cavitation. The basic idea of this paper is to find a way of increasing towing velocity in cavitation flow regime. If this can be achieved, many cavitation experiments, that are difficult or impossible in water tunnels, will be able to be done in towing tanks.

2. SYSTEM OF THE TOWING TANK

2.1. Description of the tank

Figure 1 shows the schematic front view of the experimental facility. A water tank (2) with inner sizes of 1.14m×1m×50mm is inserted into a frame constructed by four vertical steel columns (7). The tank

(2) is placed on the bottom plate (9) and is covered by an upper plate (1). The tank is fixed with the upper and bottom plates by fixing L-steel (8). The connection of the vertical steel columns (7) and the bottom plate (9) is reinforced by strengthening sheet (10). The lower part of the vertical steel columns (7) is fixed by tripod (14), and at the bottom of the tripod (14) installed with foot wheel (11). There are two flange holes (6) above and below the tank, used as water inlet and water outlet respectively, and the lower flange hole is connected with a ball valve (13) to control its opening and closing. The front wall of the tank is windowed with a 1.14m×390mm plexiglass plate (3) for flow visualization. A VW-6000 high speed camera system (KEYENCE Co. Ltd., Japan) (4) & (5) with a maximum frame rate of 4000 Hz is applied to do the visualization. According to different conditions, 2 to 4 lighting lamps (12) are used as light source and each lamp has 1300 W power.

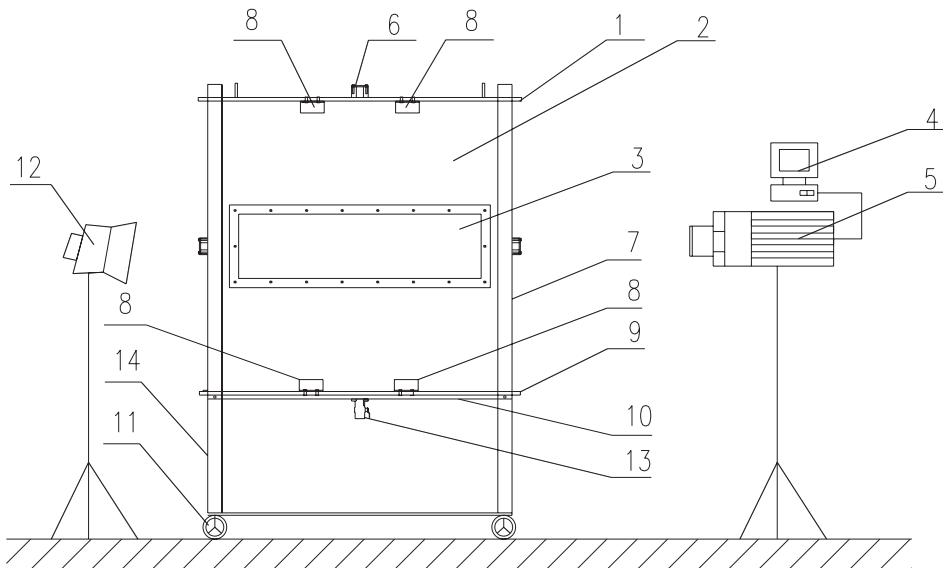


Fig. 1 Schematic of front view of the 2D high speed towing tank. (1) upper cover plate; (2) water tank; (3) plexiglass window; (4) control computer; (5) high-speed camera; (6) flange hole; (7) steel column; (8) fixing L-steel; (9) bottom plate; (10) strengthening sheet; (11) foot wheel; (12) lighting lamp; (13) ball valve; (14) tripod.

Figure 2 shows the schematic back view of the experimental facility. Just opposite the plexiglass plate (3), there is a steel plate (15) with the same size, and a motion groove (16) whose width is 12 mm is grooved in the middle of the steel plate (15). The motion groove (16) connects with the tank (2). At the symmetrical positions of both sides of the motion groove (16) are provided with two guide rails (23), a small vehicle (19) equipped with 4 wheels which are ball bearings (27) moves along the two guide rails (23). The motion power is provided by two springs (22) which connect with the vertical steel column (7) that next to the end of the motion groove (16). Each spring can provide a maximum tensile force of about 130 kg. After traveling through the groove, the high-speed vehicle is stopped by a cushioning pad (21) that is made by overlapping a tendon pad and a hard spring, which is installed at the end of the motion groove (16). Two protection plates (20) are fixed on the steel plate (15) and cover the wheels to insure that the ball bearings (27) are in the guide rails. On the vertical steel column (7) that next to the starting position of the motion groove (16), is equipped with a launch trigger (18) and two pulleys (17). The launch trigger (18) arranged coaxially with the motion groove (16) is used to launch the vehicle (19). Figure 3 shows how the launch trigger (18) clasps the small vehicle (19); the two pulleys (17) are used to pull the vehicle (19). Fig. 4 shows a photo of the experimental facility.

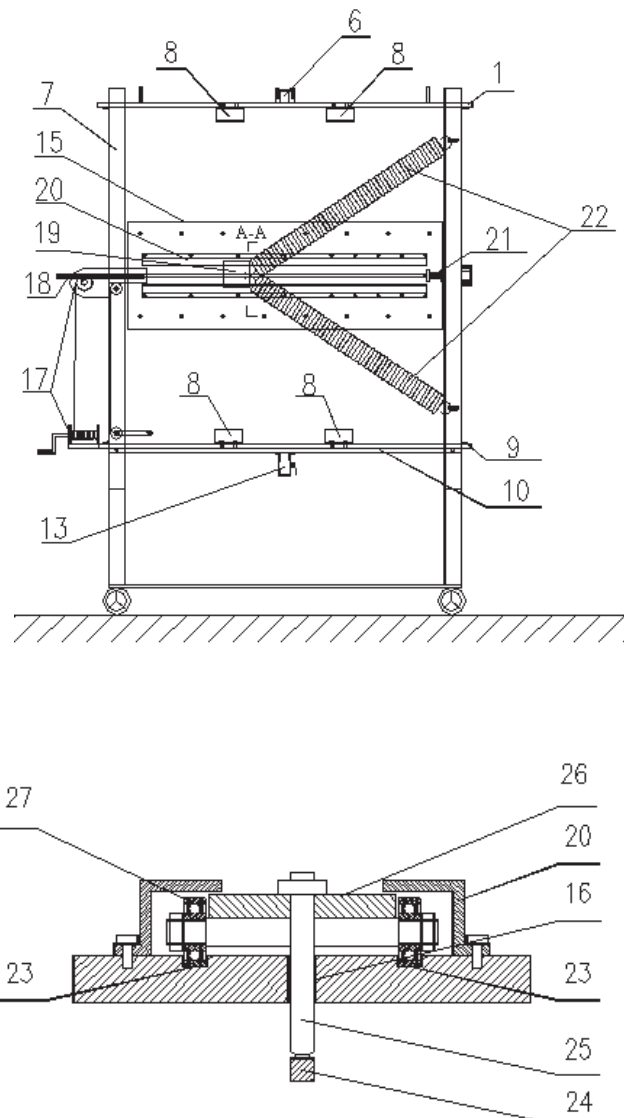


Fig. 2 Schematic of back view of the 2D high speed towing tank. a complete back view; b the sectional view of the cross-section A-A. (15) steel plate; (16) motion groove; (17) pulley; (18) launch trigger; (19) small vehicle; (20) protection plate; (21) crash pad; (22) spring; (23) guide rail; (24) experiment model; (25) connection rod; (26) vehicle body; (27) ball bearing.

Figure 3 also shows the arrangement of the small vehicle (19). The four ball bearings (27) are installed on the two ends of two bearing connecting rods (29). The vehicle body (26) is arranged on the two bearing connecting rods (29). At the center of the vehicle body (26), a connection rod (25) is installed, and the experiment model (24) is fixed on the end of the connection rod (25). The model (24) inserts into the water tank (2) via the motion groove (16). The vehicle body (26) has been bored two traction holes (28) to connect two springs (22), and one reset hole (30) to connect traction rope. Still, there is a starting baffle plate (31) on the vehicle body (26), used to fasten the vehicle (19).

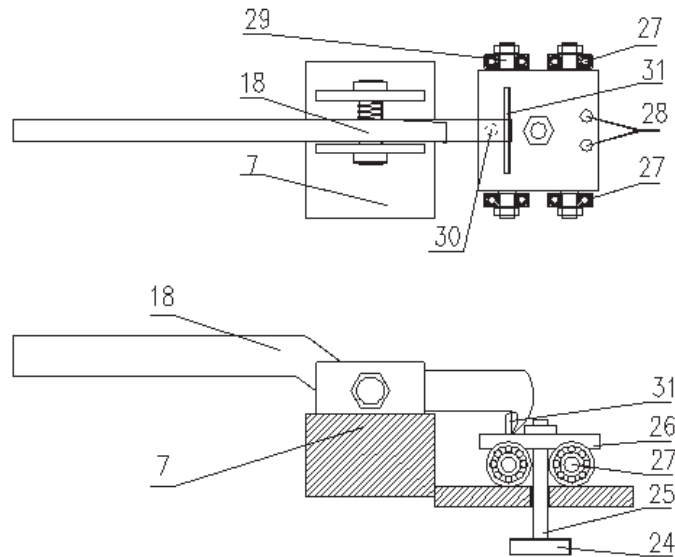


Fig. 3 Schematic of the launch trigger (18) claspsing the vehicle. a vertical view; b side view. (28) traction hole; (29) bearing connecting rod; (30) reset hole; (31) starting baffle plate.



Fig. 4 Photo of the experimental facility

2.2. Experimental procedure

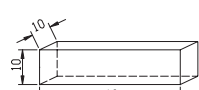
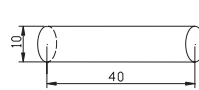
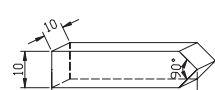
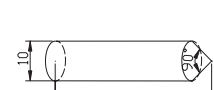
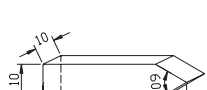
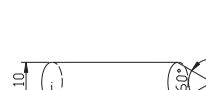
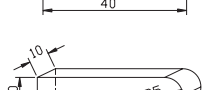
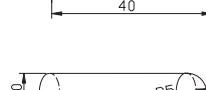
After fixing the whole facility, a traction rope fixed in the reset hole (30) of the vehicle (19) and pull the vehicle (19) to the starting position of the motion groove (16) via the two pulleys (17). Then engage the hook of the launch trigger (18) in the starting baffle plate (31) to clasp the small vehicle (19). Seal the motion groove (16) with sticky tape. After that, adjust the location, the focus, the frame speed and so on of the high speed camera to ensure that the pictures are clean. Fill the tank (2) with water to the desired level, turn on the lighting lamps, cast off the traction rope that fixed in the reset hole (30). At last, release the launch trigger (18), the small vehicle (19) shot out instantaneously, and carries test model that submerged in water through the motion groove (16). The high speed camera takes the movement pictures of the model and stores them in the computer in the form of digital images.

3. RESULTS AND DISCUSSIONS

To test the hydrodynamic characteristics of the high-speed towing tank, two groups of test models with square and circular cross-sectional areas were applied. The detailed geometries of the models are shown in Table 1. All the models are made from steel. They were coated using red paint to distinguish

boundary of cavities. Our design allows the impact of the towing vehicle with the tank. Therefore, after the experiments, the entire device system is intact. This means the towing-tank is very durable.

Table 1 Geometry of the test models

Head shape	10mm length square	10mm diameter circle
Flat		
90° taper angle		
60° taper angle		
Round		

3.1. Velocity

The frame rate of high speed camera is 1000 Hz, so the time interval Δt between two adjacent pictures is 1 ms, we measured the displacement Δx of the model in two adjacent pictures, and the instantaneous velocity can be calculated as follows:

$$v_x = \Delta x / \Delta t \quad (2)$$

The uncertainty in the velocity measurement is within $\pm 2\%$ [6].

Figure 5 collects the velocity data against displacement of the four models of square cross-section. It is seen that within the distance of 30 cm, the models have been accelerated to 12~15 m/s. When displacement X is less than 13 cm, the velocities of the four models are generally coincident. When X is greater than 13 cm, velocity curves become divergent. The velocity of the flat head one oscillates most significantly. At this stage, the velocity of the round head one is the lowest and oscillates little. This means that the motion of the round head one is stable. The velocities of the models with 60° and 90° taper angles reach high values and keep relatively stable. Therefore, the present experiment demonstrates that these two models have good hydrodynamic behaviors.

Figure 6 shows the measured velocities against displacement of the four models with circular cross-section. It is also seen that at the distance of 30 cm, the models have been accelerated to 14 m/s. Although the velocity is somewhat less than that of a square cross-sectional one, the four models' velocity curves are more coincident and smooth. This may suggest that in the towing tank that we designed, a circular cross-sectional model may have a better performance.

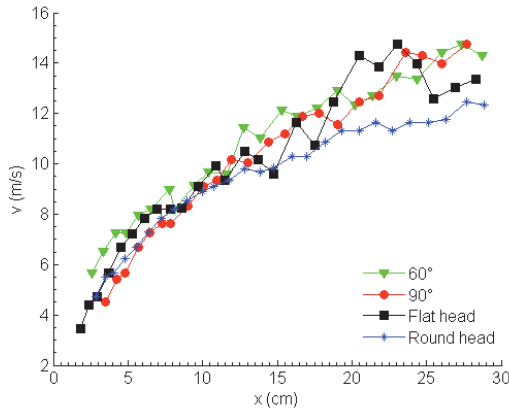


Fig. 5 Measurement results of the velocities of four square cross-sectional models along the displacement.

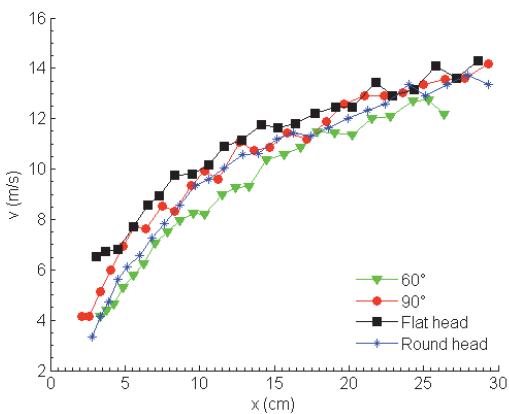


Fig. 6 Measurement results of the velocities of four circular cross-sectional models along the displacement.

Figure 7 shows the whole movement velocity of part of the models. It is seen that the accelerating section of the towing tank is from 1–60 cm, and the maximum tow speed can reach about 18 m/s, and in the section of 60–80 cm, the velocity maintained at a higher value, then the velocity began to decline somewhat. This shows that the towing tank works well and is very effective.

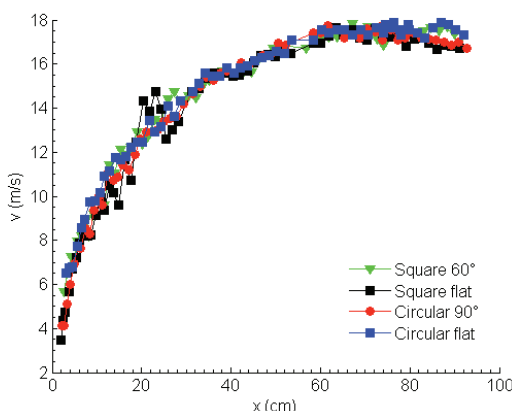


Fig. 7 Measurement results of the velocities of two square and two circular cross-sectional models along the whole displacement.

3.2. Cavitation wake

The drag force acting on an underwater body is related to body's head shape, cross-sectional shape as well as the cavitating wake [7]. In all the experiments, the cavitating wake phenomenon appeared. This means that the towing tank can be used to do cavitation experiments. In order to quantitatively describe the cavitating wake, we define a parameter $c = a/b$, where a is the cavitating wake length and b is the cavitating wake width, as shown in Fig. 8. Actually, the parameter c represents the ratio of length to diameter. In the following, according to the high-speed photographs, the parameters a , b and c of various test models are given.

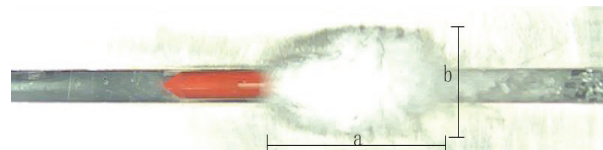


Fig. 8 Definition of the size of the cavitating wake. The red area is the steel test model. Model: circular 90°

Figure 9 shows the length to diameter ratios of four square cross-sectional models vs. velocity. It is seen that the length to diameter ratios increase with velocity in their own slope. Among them, the round one obtains the highest ratio c , which means that its wake is most slender. The 90° one has the lowest ratio, which means that its wake is stumpy.

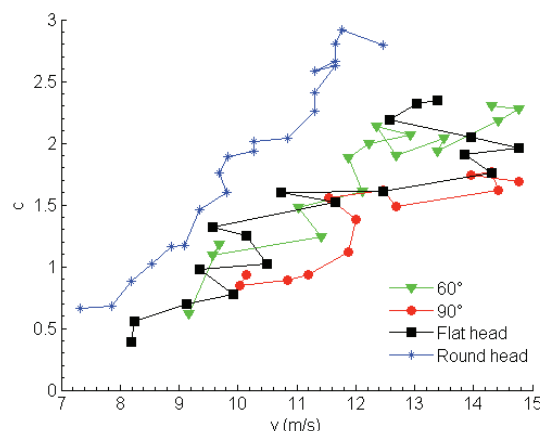


Fig. 9 Length to diameter ratios of the cavitating wakes of square cross-sectional models vs. velocity.

For clarifying the difference in the wakes, Fig. 10 gives the relationship between the wake length a and the wake width b . In the figure, the vertical axis is a and the horizontal axis is b . It is seen that when b is small, that is, at the initial stage of the cavitating wake development, the wake lengths of the four models are quite close. When b is greater than 50 mm, the wake length of the round one grows mostly fastest. That is why its wake is most slender. The 90° one gets a shortest wake length.

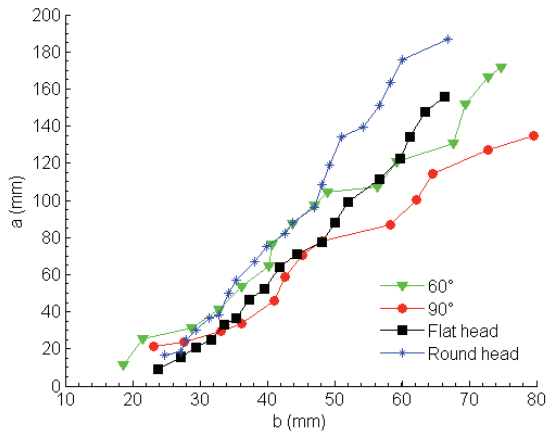


Fig. 10 Relationship between the wake length and the wake width of the square cross-sectional models.

Figure 11 shows the relationship between the length to diameter ratio and the velocity of the four circular cross-sectional models. From the figure, it is known that at the same velocity, namely at the same downstream distance (see Fig. 6), the wake's shapes of the four models are different. The wake of the 60° one is most slender whereas the wake of the 90° is most stumpy. By ignoring the specific downstream position and velocity, the data of a and b of the four cavities are collected in Fig. 12. The function of Fig. 12 is to see that once the wakes reach a same width, whether their lengths are different. We find that the wakes' shapes eventually reach similarity. This kind of similarity does not exist for the square cross-sectional models (see Fig. 10). The reason for this may be attributed to flow instability and non-linear vortex generated at the four corners of a square cross-sectional model [8].

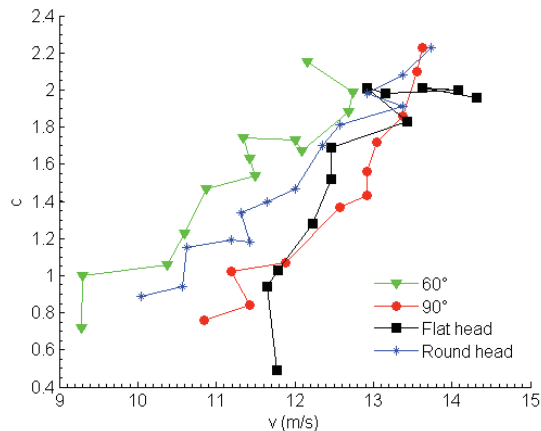


Fig. 11 Length to diameter ratios of the cavitating wakes of circular cross-sectional models vs. velocity.

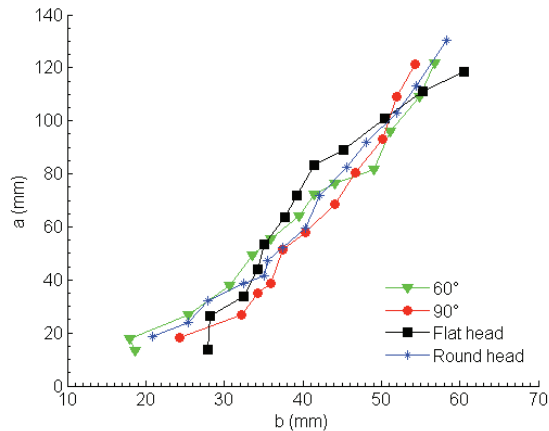


Fig. 12 Relationship between the wake length and the wake width of the circular cross-sectional models.

3.3. Effect of cross-section geometry on the wake cavity

Figure 13 compares the wake shape caused by a 90° square model with that caused by a 90° circular model. When the cavities in the two cases reach a same width b , the length of the cavity a caused by the square model is longer and the cavity shape is close to a cone. The length of the cavity a caused by the circular model is shorter and the cavity shape is close to a cylinder.

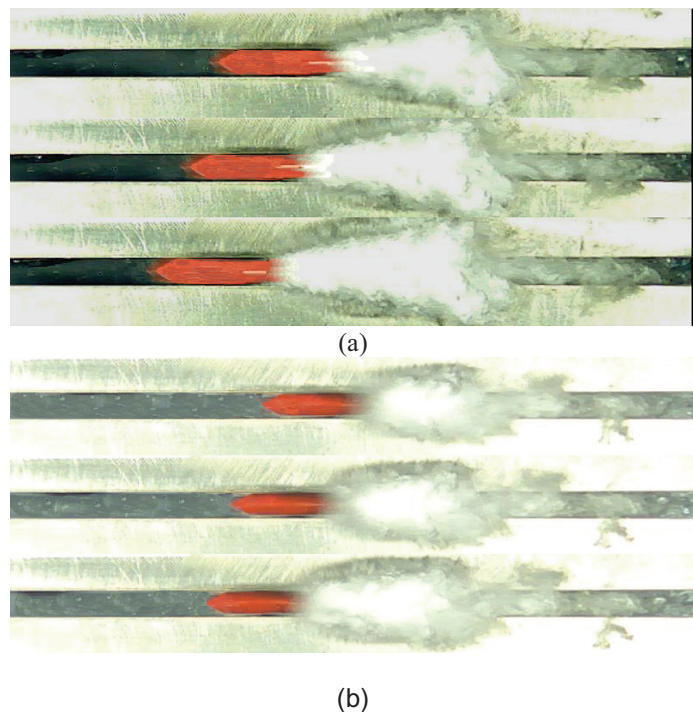


Fig. 13 Comparison of the wake's shapes of 90° models. a square cross-section; b circular cross-section. The models (red area) move from the right to the left.

4 CONCLUSIONS

- (1) A new type of high speed towing tank has been successfully developed at our laboratory. Within the distance of 30 cm, the test models can be accelerated to about 14-15 m/s. The maximum tow speed can reach about 18 m/s. Our work demonstrates that the idea can be applied to towing tanks of larger scale.
- (2) Through the test of 8 models, it has been found that the hydroballistic behavior and the shape of the wake cavity for the model are related to the shape of the model.
- (3) In the towing tank, one experiment only takes a time of less than 70 ms while the water leakage from the motion groove starts after a few seconds due to the inertia of water. This is to say that the flow fields observed in this experiment are not influenced by other factors.

ACKNOWLEDGEMENTS

This work was supported by the Zhejiang Provincial Natural Science Foundation, China, under a priority project (Grant No. Z1110123) and by Science Foundation of Zhejiang Sci-Tech University (ZSTU), China. The authors gratefully acknowledge these sources of support. The authors would also like to thank the assistance in experiments by Miss Su-Yun Zhou, Mr. Xiao-Dong Zhang, Assoc. Profs. Ruo-Ling Dong and Li-Te Zhang. Part of this paper was orally presented at the 8th International Symposium on Cavitation, 13-16 August 2012, Singapore.

REFERENCES

- [1] Ashley, S., 2001, "Warp Drive Underwater," *Scientific American*, 17, pp. 70–79.
- [2] Trevena, D. H., 1987, *Cavitation and Tension in Liquids*, Taylor & Francis, Bristol.
- [3] Etter, R. J., Cutbirth, J. M., Ceccio, S. L., Dowling, D. R., Perlin, M., 2005, "High Reynolds Number Experimentation in the US Navy's William B Morgan Large Cavitation Channel," *Meas Sci Technol.*, 16, pp. 1701–1709.
- [4] Techet, A. H., Hover, F. S., Triantafyllou, M. S., 1998, "Vortical Patterns Behind a Tapered Cylinder Oscillating Transversely to a Uniform Flow," *J Fluid Mech.*, 363, pp. 79–96.
- [5] Cui, J. Z., 1995, "A Study on Characteristics of Six Panel Demersal Trawl Nets," *J Fisheries China*, 19(1), pp. 43–51. (in Chinese)
- [6] Zhang, X. P., 2012, "Development of a High-Speed Towing Tank and Experimental Study of Hydrodynamics and Cavitation of Different Geometric Models," Master Thesis, Zhejiang Sci-Tech University, China. (in Chinese)
- [7] Knapp, R. T., Daily, J. W., Hammitt, F. G., 1970, *Cavitation*. McGraw-Hill, New York.
- [8] Shi, H. H., Wang, X. L., Ito, M., Koshiyama, K., Huang, Z., 2001, "Unsteady Liquid Jet Flowing through a Rectangular Nozzle," *Experiments and Measurements in Fluid Mechanics* 15(2), pp. 59–70.